CIRP Journal of Manufacturing Science and Technology 50 (2024) 65–79

Contents lists available at ScienceDirect

CIRP Journal of Manufacturing Science and Technology

journal homepage: www.elsevier.com/locate/cirpj

Full-length article

Parameters optimization for chatter-free milling tool path based on spindle speed variation method

Min Wan [a,*], Xue-Bin Qin [a], Jia Dai [a], Wei-Hong Zhang [a], Xiao-Ling Sun [b]

[a] State IJR Center of Aerospace Design and Additive Manufacturing, School of Mechanical Engineering, Northwestern Polytechnical University, Xi'an, Shaanxi 710072, China

[b] Xi'an Aerospace Power Machinery Co.,Ltd., Xi'an, Shaanxi 710025, China

A R T I C L E I N F O

Keywords:
Spindle speed variation
Parameter optimization
Chatter suppression
Shortest tool path

A B S T R A C T

Existing methods orienting for optimizing cutting parameters in milling process with spindle speed variation (SSV) only optimally selected the axial depth of cut and only considered the acceleration constraint of spindle. This article proposes a systematic optimization method to obtain the best combination of multiple machining parameters (axial and radial depths of cut) and SSV's parameters (the ratio of variation amplitude and the ratio of variation frequency) so that the chatter-free milling tool path can be shortened. Both acceleration and jerk constraints of spindle are considered. A C^3 continuous variable feedrate scheduling algorithm is used to eliminate the influence of spindle speed variation on feed per tooth, which is thus not required to treat as an optimization variable. The machining parameters of each iterative step are updated by following that the number of axial and radial cutting layers could be decreased. Discrete optimization method is combined with chatter stability analysis to solve the problem. A series of milling experiments verify that the proposed method can achieve the shortest tool path with chatter-free condition.

1. Introduction

Machining chatter is a common vibration phenomenon, which can destroy the machined surface and reduce the tool life. In recent years, many studies focused on establishing chatter-free machining methods with high productivity, such as selecting optimal machining parameters from stability lobe diagrams (SLDs) [1,2], suppressing chatter through the cutting-induced process damping [3] and enhancing the maximal axial depth of cut (ADC) by changing the helix angle of tool [4]. Among these, a periodical spindle speed variation (SSV) method, which can disrupt the phase relationship between the inner and outer modulations of machined surface, is widely used to suppress the aggregation of chatter and simultaneously improve the stable axial depth of cut [5,6].

Many scholars focused on developing different SSV-based methods to suppress machining chatter with the performance improvement. Seguy et al. [7] used SSV to suppress chatter occurring in high-speed milling, and summarized that the stability can always be improved when the speed is in the domain of the first flip (period doubling) lobe. Hajikolaei et al. [8] combined SSV with an active controller to quickly suppress the chatter. By using the periodic speed variation, Kong et al. [9] used various chaotic signals to overcome the beat vibration occurring in machining. Jin et al. [10] combined SSV with variable pitches and phases to improve the chatter suppression effect. For the purpose of obtaining the optimal cutting parameters, Ding et al. [11] proposed an active chatter suppression system to simultaneously adjust the amplitude and frequency parameters according to a fractional-order proportional integral differential (FOPID) controller. Besides, Niu et al. [12] proposed a variable-step numerical integration method to decrease the calculation load of stability analysis with SSV, while Dong et al. [13] utilized a reconstructed semi-discretization method to efficiently analyse the stability of the machining processes with SSV.

It is well recognized that parameter optimization, which involves chatter avoidance problems, is an important topic for improving the machining performance and quality [14–19]. For example, to maximize material removal rate (MRR) and avoid the appearance of forced vibration and chatter, Ringgaard et al. [20] used a penalty cost function to optimize the machining parameters of thin-walled structures. Tang and Liu [16] drew a three-dimensional lobe diagram, which covers spindle speed, axial and radial depths of cut, to choose the optimal machining parameters for maximizing MRR of thin-wall end milling. Ozoegwu et al. [17] proposed an optimization method to minimize the pocketing time of a zigzag toolpath. Kumar and Singh [18] used the response surface methodology to develop a chatter-free optimization model for turning, and then adopted a multi-objective genetic algorithm technique to solve the stable cutting zone with the maximized

* Corresponding author.
E-mail address: m.wan@nwpu.edu.cn (M. Wan).

https://doi.org/10.1016/j.cirpj.2024.02.006
Received 16 October 2023; Received in revised form 24 January 2024; Accepted 18 February 2024
Available online 27 February 2024

MRR. Based on a self-learning algorithm, Bergmann and Reimer [19] proposed an online adaptive optimization method to automatically adjust the milling parameters. Deng et al. [21] proposed a machining parameters optimization method for a multi-pass milling by considering multi objectives such as cutting time and surface roughness. Harun [22] used a Taguchi design method to find the optimal parameters of a turning process based on the measured MRR, roughness, sound intensity, energy consumption, and vibration signals. To improve the machining efficiency, Zhang et al. [23] proposed an efficient parameter optimization method by combining an off-line optimization with a real-time monitoring of multi-signals such as cutting forces, spindle torque and power.

It is worth pointing out that although above existing optimization methods have achieved great advancements in their touching fields, they mainly focused on the processes with constant spindle speed, and did not touch the optimization of SSV. Actually, also aimed at chatter suppression and productivity improvement, SSV-based parameter optimal selection also attracted a little attention for milling process. For example, Seguy et al. [24] simulated the critical axial depths of cut under different SSV parameters, i.e. the ratio of variation amplitude (RVA) and the ratio of variation frequency (RVF), by considering the kinematic constraints of spindle, and then optimally selected the SSV parameters to increase the axial depth of cut. By analysing the machining performance of SSV with different variation modulations and speeds, Niu et al. [12] also realized the selection of optimal SSV parameters under the acceleration constraint of spindle. Wang et al. [25] utilized genetic algorithm to optimize the SSV parameters of a multi harmonic spindle speed variation method, and improved the critical axial depth of cut for high-speed milling. In summary, these works mainly focused on optimally selecting SSV parameters to increase the critical depth of cut without chatter, however, other machining parameters, such as radial depth of cut (RDC) and feed per tooth, were not involved in these works.

Actually, SSV-involved optimization methods still can be improved by considering more parameters, such as radial depth of cut and feed per tooth, together with the constraints of parameters range. Hence, this article proposes a discrete parameter optimization method to comprehensively determine SSV parameters (RVA and RVF) and machining parameters (ADC, RDC and feed per tooth). Compared to existing methods, the main advantages of this work are as follows.

- The existing methods [12,24] only optimized the SSV parameters (i.e. RVA and RVF) and axial depth of cut (ADC). However, besides these three parameters, another important parameter, i.e. the radial depth of cut (RDC), is also included in the optimization procedure of the proposed method.
- The optimization objective of existing SSV methods [12,24] is only to maximize ADC, and thus, the total machining trajectory cannot be necessarily minimized. The proposed method aims at establishing an optimization algorithm to obtain the shortest machining trajectory by comprehensively considering ADC, RDC and the total material volume to be removed.
- For the optimization procedure, the machining parameters of each iterative step are updated by following that the number of axial and radial cutting layers could be decreased. Compared with the existing methods [12,24] that need to calculate the maximum ADC for each set of SSV parameters, this rule can greatly reduce the calculation load, especially for the stability analysis related to SSV.

Finally, a variable feedrate scheduling method proposed in Ref. [26] is successfully used to decouple the connection between the feed per tooth and SSV parameters. It eliminated the necessity of optimizing feed per tooth without lowing machining productivity.

This article is organized as follows. The optimization method is introduced in Section 2, which includes the determination of optimization parameters, the establishment of optimization objective and the construction of optimization procedure. In Section 3, a series of milling experiments are designed with two types of workpieces, i.e. an inclined table workpiece and a pocketing workpiece. It is verified that the proposed optimization algorithm is effective for improving machining productivity, and at the same time, the optimized machining parameters obtained by the proposed algorithm are integrated into some milling tests to verify the chatter suppression effectiveness of the method. Section 4 is the summary of this article.

2. Optimization of the machining parameters and spindle speed variation parameters

In contrast to the existing SSV-related researches that only optimally selected the axial depth of cut, both axial and radial depths of cut are defined as optimization parameters in this work. The actual length of tool path is set as an optimization objective to improve the productivity. Then an optimization procedure is established based on the principle that the scheduled tool path can be shortened as much as possible according to the total material volume of the designed cutting area. Finally, an open-architecture CNC machine tool, which is specifical for realizing the SSV-based optimal machining process, is established and developed for verification.

2.1. The determination of optimization parameters and the establishment of optimization objective

The spindle speed in relation to the machining process with SSV follows a periodical variation, e.g. triangular modulation or sinusoidal modulation, to realize chatter suppression. Due to the characteristic of high-order continuity, the sinusoidal curve is used to schedule the spindle speed variation. Based on this idea, the variable spindle speed $\Omega(t)$ can be expressed as follows.

$$\Omega(t) = \Omega_0 + \Omega_A \sin(\omega t) \tag{1}$$

where Ω_0 is the average of spindle speed. Ω_A and $\frac{\omega}{2\pi}$ are the amplitude and frequency of speed variation. ω is angular velocity. The modulation parameters of spindle speed variation, i.e. RVA and RVF, are expressed as follows.

$$\begin{cases} \text{RVA} = \dfrac{\Omega_A}{\Omega_0} \\ \text{RVF} = \dfrac{30\omega}{\pi\Omega_0} \end{cases} \tag{2}$$

Because RVA and RVF determine the performance of chatter suppression, they are the required parameters to be optimized for the process with SSV. Besides these parameters, ADC and RDC, i.e. a_p and a_e, which directly influence the machining efficiency, are another set of parameters needing to be optimized.

It is pointed out that the constant feedrate will result in the variation of feed per tooth, which is related to RVA, as shown in Fig. 1. Based on this fact, the variable feed per tooth is usually at a relatively low level so that the constraint of maximum feed per tooth can be guaranteed. Correspondingly, the machining efficiency is not maximized even if the machining trajectory is the shortest. It can be found that the relationships of constant feedrate v_c, variable feed per tooth $f(t)$ and variable spindle speed $\Omega(t)$ can be expressed as follows.

$$\begin{cases} v_c = \dfrac{f_{\max} N \Omega(t)_{\min}}{60} = \dfrac{f_{\max} N \Omega_0}{60}(1 - \text{RVA}) \\ f(t) = \dfrac{60 v_c}{N \Omega(t)} = \dfrac{60 v_c}{N \Omega_0 (1 + \text{RVA} \sin(\omega t))} \end{cases} \tag{3}$$

where N is the number of teeth, and $f_{\max}$ is the constraint of feed per tooth. If the amplitude parameter RVA is very high, the feedrate must be decreased so much that the maximum feed per tooth cannot exceed the maximum constraint. Hence, feed per tooth also needs to be considered if SSV is carried out with constant feedrate.

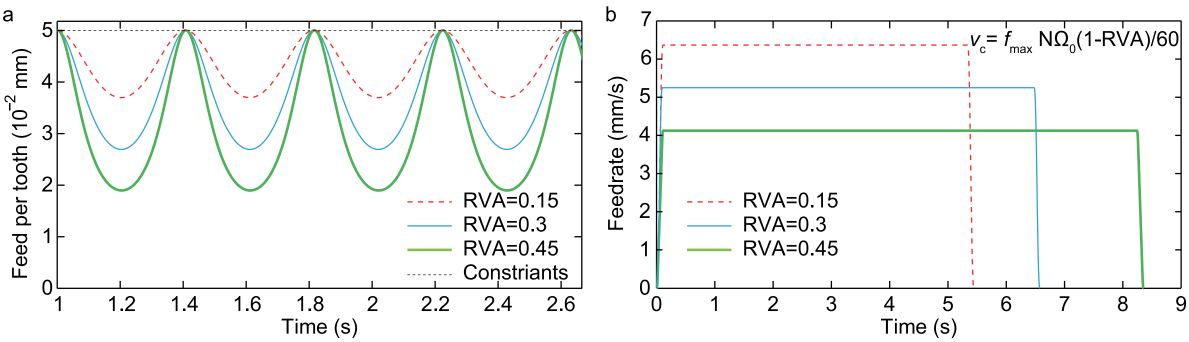

Fig. 1. The feed per tooth and feedrate scheduling results for SSV with constant feedrate. (a) The feed per tooth with different RVA; (b) the maximum constant feedrate with different RVA for the same trajectory.

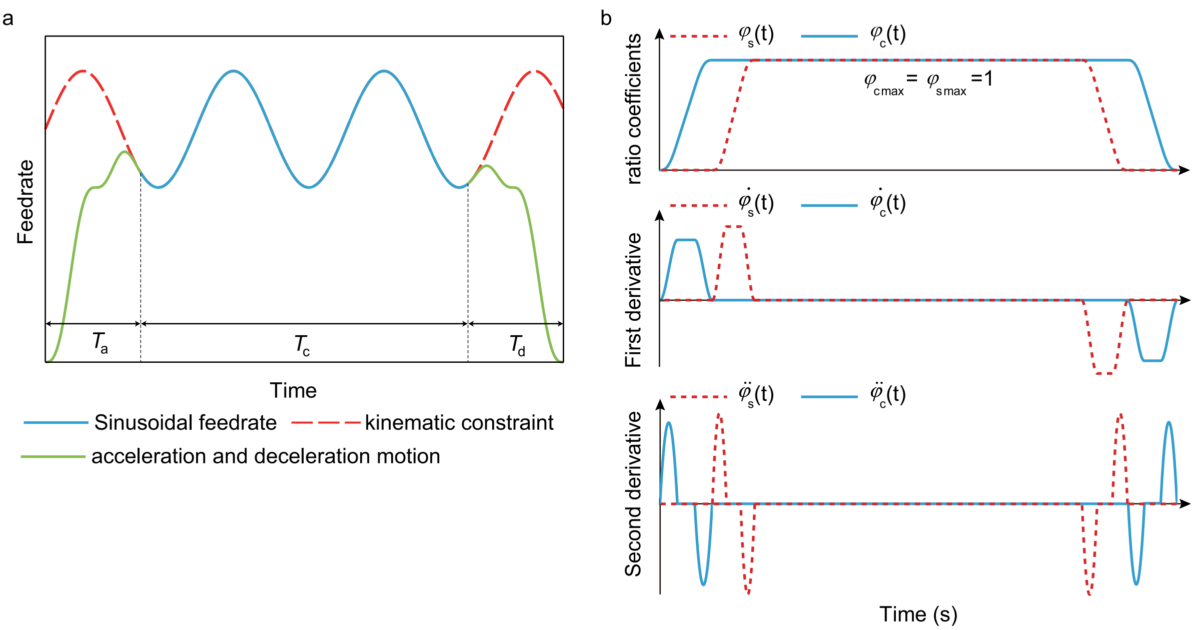

Fig. 2. The sinusoidal feedrate scheduling based on the method reported in Ref. [26]. (a) The actual velocity scheduled results and (b) the scheduled profile of ratio coefficients.

To eliminate the variation of feed per tooth resulting from SSV, the C^3 continuous feedrate scheduling method proposed in Ref. [26] is used to produce a variable feedrate to match the variable spindle speed. The scheduled feedrate $v(t)$ is shown in Fig. 2a and expressed as follows.

$$v(t) = \varphi_c(t) f_{max} N\Omega_0(1 - \mathrm{RVA}) + \varphi_s(t) f_{max} N\Omega_0 \mathrm{RVA}(\sin(\omega t + \theta) + 1) \quad (4)$$

where θ is the extra phase angle to guarantee that the scheduled feedrate can match the variable spindle speed. The scheduled feedrate is divided into two parts, i.e. the constant speed and the extra sinusoidal speed. $\varphi_c(t)$ and $\varphi_s(t)$ are the time-varying ratio coefficients for the two parts, respectively, and the scheduled results of them are shown in Fig. 2b.

Eq. (4) actually ensures that the feed per tooth keeps constant during the process with SSV. In other words, feed per tooth is not a mandatory optimization parameter when the variable feedrate is adopted. Hence, the main task of optimization can be divided into two parts: one is to find a suitable group of RVA and RVF to achieve the chatter-free milling, and the other is to find the optimal combination of a_p and a_e to guarantee the optimal machining efficiency. Instead of simply pursuing for the maximum axial depth of cut like the existing works, the objective is set as the shortest tool path to improve the machining productivity. Actually, the total length of machining trajectory directly influences the actual machining efficiency. By comprehensively considering the influence of three key aspects, i.e. ADC, RDC and the total material volume to be removed, this article aims at establishing an optimization algorithm to obtain the shortest machining trajectory so that the total machining time can be minimized. However, the optimization objective of existing SSV methods is only to maximize ADC. This kind of treatment cannot balance ADC and RDC, and easily leads to the underutilization of depth of cut on the last cutting layer. As a result, the total machining trajectory together with the corresponding machining time cannot be necessarily minimized since additional cutting layer needs to be removed.

In summary, the proposed optimization method considers the influences of machining parameters (i.e. ADC and RDC), SSV parameters (i.e. RVA and RVF), the length of machining trajectory (optimization objective) and the influence of feed per tooth, and the optimization problem is formulated as follows.

$$\begin{aligned} &\text{minimize} && F = \sum_{i=1}^{m} \sum_{j=1}^{n} L_{i,j}(a_p, a_e, \mathrm{RVA}, \mathrm{RVF}) \\ &\text{subject to} && a_e \le D \\ &&& (\mathrm{RVA}, \mathrm{RVF}) \in \Gamma(\Omega_0, A_{max}, J_{max}, A_{s\,max}, J_{s\,max}) \\ &&& \max(|\lambda|) < 1 \end{aligned} \quad (5)$$

where F is the optimization objective function. m is the number of axial cutting layers under a_p, and n is the number of radial cutting layers with a_e for the ith axial layer. $L_{i,j}$ is the length of the jth radial layer for the

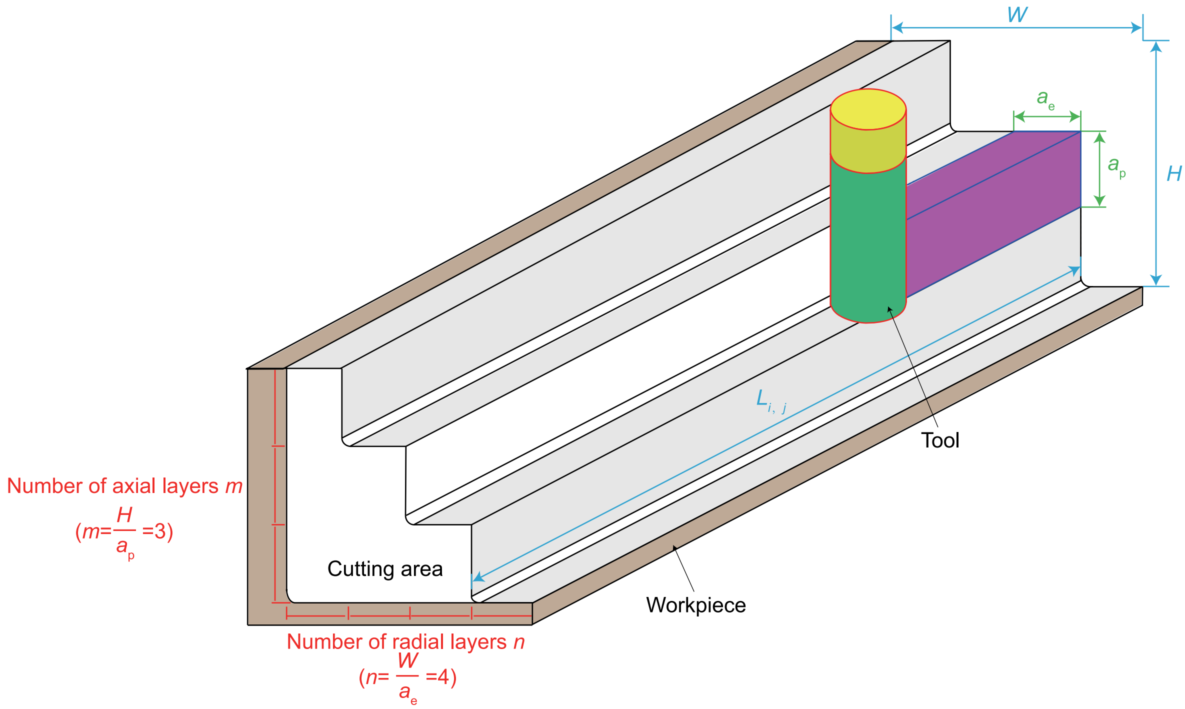

Fig. 3. The diagram of workpiece with m axial cutting layers and n radial cutting layers.

ith axial layer, as shown in Fig. 3, where H and W are the height and width of cutting area, respectively, and the following relationship needs to be satisfied.

$$\begin{cases} m = \dfrac{H}{a_\mathrm{p}} \\ n = \dfrac{W}{a_\mathrm{e}} \end{cases} \tag{6}$$

D is the diameter of mill. Γ is the permissible range of SSV parameters depending on the average spindle speed Ω_0 and the kinematic constraints of motion axes and spindle. $A_{\max}$ and $J_{\max}$ are the maximum acceleration and maximum jerk of the feedrate, respectively. $A_{\mathrm{s}\max}$ and $J_{\mathrm{s}\max}$ are the maximum acceleration and maximum jerk of spindle, respectively. λ is the eigenvalue of transition matrix $\boldsymbol{\Phi}$ for stability analysis, which is used to judge the occurrence of chatter or not. The construction of transition matrix $\boldsymbol{\Phi}$ can be founded in Ref. [27]

The specific expression for SSV parameters range Γ can be expressed as follows:

$$\begin{cases} 0 < \mathrm{RVA} \cdot \mathrm{RVF} < \dfrac{30\sigma\eta A}{\pi\Omega_0^2} \\ 0 < \mathrm{RVA} < \dfrac{30\sigma}{\pi \mathrm{RVF}\Omega_0^2}\sqrt{\dfrac{\eta^2 A^2}{2} + \sqrt{-\dfrac{3\eta^4 A^4}{4} + \dfrac{900\eta^2 A^2 J^2}{\pi^2 \mathrm{RVF}^2 \Omega_0^2}}} \end{cases} \tag{7}$$

with

$$\begin{cases} \eta = 1, & \text{if } \mathrm{RVF} \le \dfrac{30J}{\pi\Omega_0 A} \\ \eta = \dfrac{30J}{\pi A\Omega_0 \mathrm{RVF}}, & \text{if } \mathrm{RVF} > \dfrac{30J}{\pi\Omega_0 A} \end{cases} \tag{8}$$

$$\begin{cases} A = A_{\mathrm{s}\max}, J = J_{\mathrm{s}\max}, & \text{if } \sigma = 1 \\ A = A_{\max}, J = J_{\max}, & \text{if } \sigma = \rho \end{cases} \tag{9}$$

where σ is the coefficient to distinguish the kinematic constraints of spindle ($\sigma = 1$) and motion axes ($\sigma = \rho$). ρ is the proportional coefficient between the spindle speed and feed motion velocity, and it depends on the maximum feed per tooth $f_{\max}$ and the number of teeth N.

$$\rho = \frac{60}{f_{\max} N} \tag{10}$$

The more detailed derivation is described in Ref. [26].

2.2. The procedure for optimizing the shortest tool path

Since the stability analysis involving SSV is based on the discrete numerical integration method proposed in Ref. [27], the discrete optimization is used for the proposed method. The general flowchart is shown in Fig. 4 and the specific optimization steps are introduced as follows.

Step1 : Obtain the initial SSV parameters set $\boldsymbol{P}_{\mathrm{ini}}$, and set the initial axial and radial depths of cut $a_{\mathrm{p,ini}}$, $a_{\mathrm{e,ini}}$.

The initial radial depth of cut $a_{\mathrm{e,ini}}$ is self-defined by considering the mill diameter and workpiece's cutting area. The corresponding critical axial depth of cut corresponding to the stable machining processes under the constant spindle speed is chosen as the initial value of axial depth of cut $a_{\mathrm{p,ini}}$. According to Eq. (7), the permissible range Γ of SSV parameters is obtained. To carry out the discrete optimization, the consecutive range Γ is dispersed into the set of uniform points like $\boldsymbol{P} = [\mathrm{RVF}, \mathrm{RVA}]$.

Step2 : Solve the optimal axial depth of cut $a_{\mathrm{p,o}}$ under the corresponding SSV parameters set $\boldsymbol{P}_w$ and radial depth of cut $a_{\mathrm{e},g}$.

The solution procedure is an iterative calculation. If the current axial depth of cut $a_{\mathrm{p},k}$ can satisfy stable machining ($\max(|\lambda(a_{\mathrm{p},k}, a_{\mathrm{e},g}, \boldsymbol{P}_w)|) < 1$), update the optimal axial depth of cut $a_{\mathrm{p,o}} = a_{\mathrm{p},k}$ and choose the next axial depth of cut $a_{\mathrm{p},k+1}$ to calculate the transition matrix's eigenvalue λ until $\max(|\lambda|) \ge 1$. To guarantee the full utilization of axial depth of cut a_p, the height of cutting area H should be divisibly divided by every chosen $a_{\mathrm{p},k}$. Combined with Eq. (6), the relationship between $a_{\mathrm{p},k}$ and $a_{\mathrm{p},k+1}$ is as follows.

$$\begin{cases} a_{\mathrm{p},k} = \dfrac{H}{m_k}, k = 1, 2, \ldots \\ \dfrac{H}{a_{\mathrm{p},k+1}} = \dfrac{H}{a_{\mathrm{p},k}} - 1 \end{cases} \tag{11}$$

where m_k is the number of axial cutting layers for the axial depth of cut $a_{\mathrm{p},k}$.

Step3 : Change SSV parameters set $\boldsymbol{P}_w$ and repeat Step 2.

For every changing of SSV parameters set, the value of a_p is not updated. Then, when all SSV parameters sets are carried out by Step 2, the current $a_{\mathrm{p,o}}$ with corresponding SSV parameters set $\boldsymbol{P}_\mathrm{o}$ is the

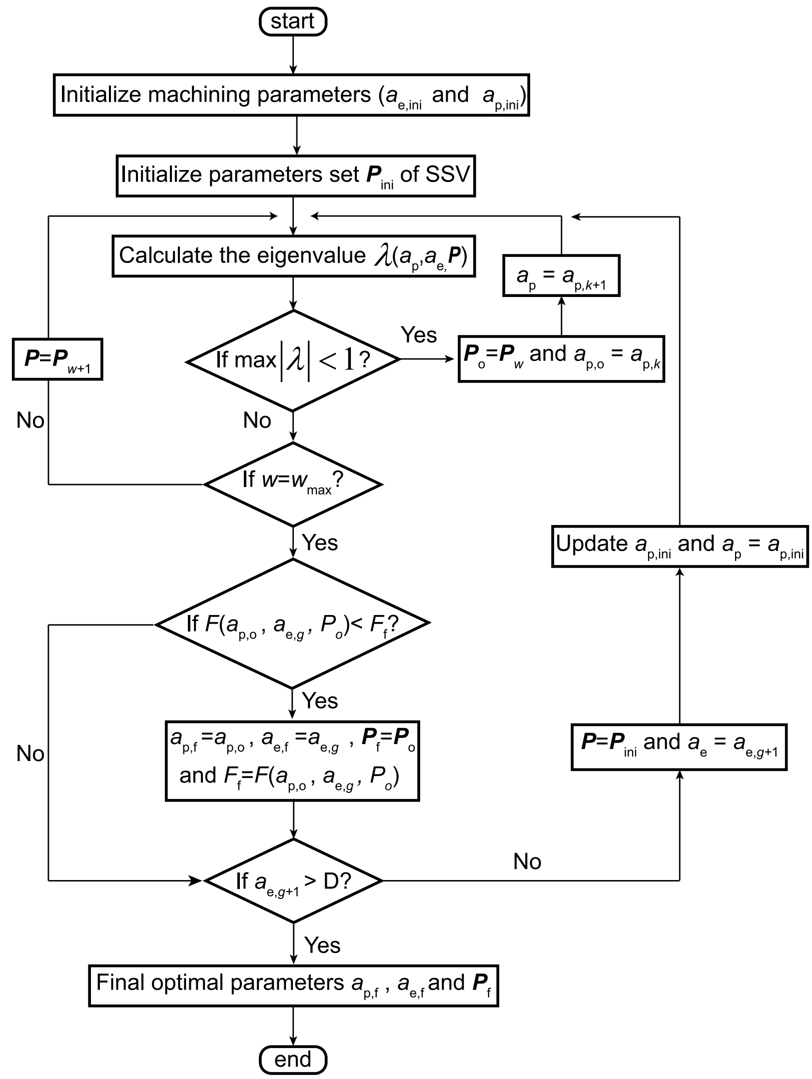

Fig. 4. The flowchart of the parameter optimization method involving SSV.

optimal selection under the specific radial depth of cut $a_{e,g}$ that can achieve the minimum value of axial cutting layers m with stable machining processes. Finally, according to Eq. (5), if the objective function $F(a_{p,o}, a_{e,g}, \boldsymbol{P}_o)$ is less than the existing optimal results $F_f = F(a_{p,f}, a_{e,f}, \boldsymbol{P}_f)$, update the final results with $a_{p,f} = a_{p,o}, a_{e,f} = a_{e,g}, \boldsymbol{P}_f = \boldsymbol{P}_o$.

Step4 : Change the radial depth of cut $a_{e,g}$, and update the initial axial depth of cut $a_{p,ini}$. Then repeat Steps 2 and 3 to find the most efficient combination of parameters.

The choice of $a_{e,g}$ is similar to $a_{p,k}$, and it aims to decrease the number of radial cutting layers n for every axial cutting layer. Combined with Eq. (6), the relationship between $a_{e,g}$ and $a_{e,g+1}$ can be expressed as follows.

$$\begin{cases} a_{e,g} = \dfrac{W}{n_g}, g = 1, 2, \ldots \\ \dfrac{W}{a_{e,g+1}} = \dfrac{W}{a_{e,g}} - 1 \end{cases} \tag{12}$$

where n_g is the number of radial cutting layers for the radial depth of cut $a_{e,g}$. As for the initial axial depth of cut to be updated, it depends on the current results and is set as the minimum value to guarantee the following relationship.

$$F(a_{p,ini}, a_{e,g}, \boldsymbol{P}_{ini}) < F(a_{p,f}, a_{e,f}, \boldsymbol{P}_f) \tag{13}$$

Finally, the whole optimization procedure will be finished when the next choice of radial depth of cut is larger than the diameter of tool ($a_{e,g+1} > D$), and the final results $a_{p,f}, a_{e,f}, \boldsymbol{P}_f$ are the optimal machining parameters and SSV parameters.

According to Eq. (11), it can be found that the step size of adjacent choices for axial depth of cut is variable and depends on the axial cutting layers and actual height of cutting area. The variable-step parameter optimization can avoid the useless improvement of axial depth of cut and ensure that every updated optimization result can directly shorten the actual tool path. For Steps 3 and 4, the choices of initial parameters also consider the results of the last optimization, which decrease the load especially in the eigenvalue calculation procedure of the transition matrix. Besides that, Eqs. (11) and (12) mainly aim at regular cutting area. For irregular cutting area, the choices of next axial and radial depths of cut depends on the actual case of cutting area, and needs to ensure that $a_{p,k+1}$ and $a_{e,g+1}$ are the minimum to achieve the reduction for the numbers of axial cutting layers m and radial cutting layers n, respectively.

3. Experimental verification

An in-house open-architecture CNC machine tool, as shown in Fig. 5, is developed to guarantee real-time synchronous variation of both the feedrate and the spindle speed. It can completely carry out

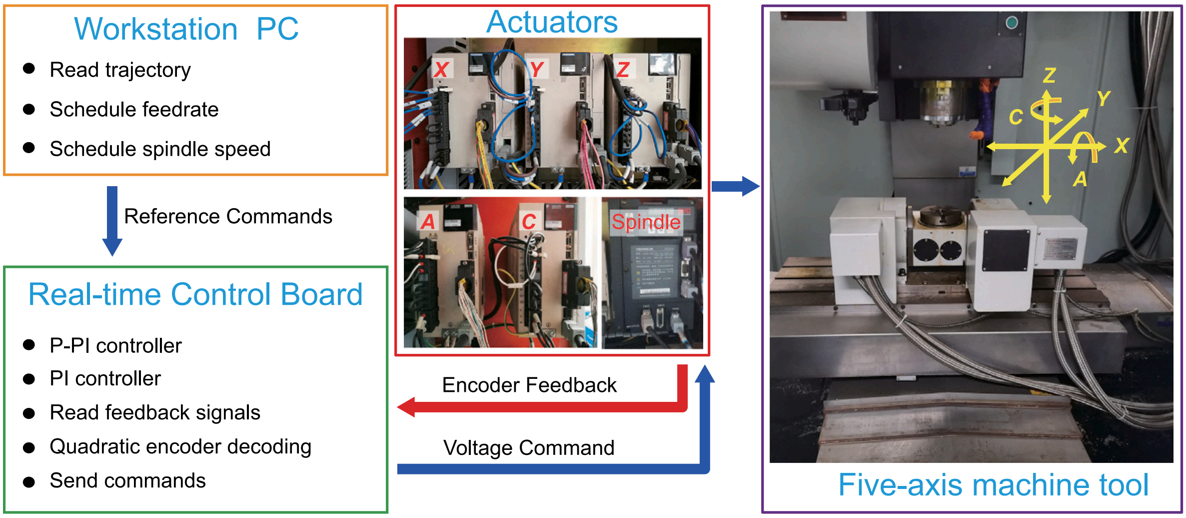

Fig. 5. The developed in-house open-architecture CNC machine tool.

Table 1
Modal parameters of the milling system.

Modal direction	Modal mass (kg)	Damping (N s/m)	Stiffness (10^7N/m)	Natural frequency (Hz)
X	0.095	18.3794	1.2904	1851.16
Y	0.094	18.0384	1.2915	1850.34

the self-designed feedrate commands of spindle and drive axes, which are obtained by the proposed optimization method. Based on this fact, SSV-based optimal milling process can be achieved.

Optimal machining parameters obtained by different optimization methods, including the proposed method and the existing method proposed in Ref. [12], are used for the same workpiece. Workpiece material is aluminum alloy Al7075. A three-fluted mill with the diameter of 8 mm and the helix angle of 45° is used in the experiments. The tangential and radial shearing force coefficients are 966.6 N/mm^2 and 411.9 N/mm^2, respectively. Modal parameters of milling system are listed in Table 1.

Furthermore, the mean spindle speed is set as 3000 rpm, which is the rated spindle speed of the machining tool. The kinematic constraints of spindle are $A_{s\,max}$ = 3000 rpm/s (acceleration constraint) and $J_{s\,max}$ = 8000 rpm/s^2 (jerk constraint). The maximum feed per tooth is 0.05 mm/tooth. The constraints of drive axes are A_{max} = 100 mm/s^2 (acceleration constraint) and J_{max} = 3000 mm/s^3 (jerk constraint). According to Eq. (7), the range of parameters RVA and RVF is shown in Fig. 6.

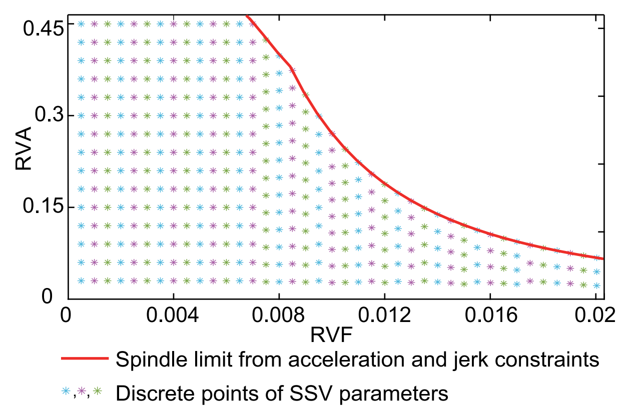

Fig. 6. The parameters range of RVA and RVF involving the influence of acceleration and jerk constraints of spindle.

3.1. Experimental verification for inclined table workpieces

Three inclined table workpieces with cylindrical bases are chosen as the first set of experiments to verify the advantage of the proposed optimization method. The cutting area of workpiece is divided into three parts, as shown in Fig. 7.

The machining parameters and the parameters of spindle speed variation are optimized by the proposed method for the three parts. The optimization results for every suitable radial depth of cut are expressed in Table 2, and the optimal parameters for every part are marked with yellow squares. As comparison, the critical axial depth of cut corresponding to the SSV's parameters is obtained based on the optimization method in Ref. [12] with a half-immersion milling. Moreover, the critical axial depth of cut corresponding to the used constant spindle speed is used for another milling to verify the enhancement of critical axial depth of cut related to SSV.

The final results of optimized machining parameters are listed in Table 3. From Table 3 it can be seen that the machining parameters obtained by the proposed method (symbolled as SSV$_O$) can achieve obvious reduction of path length than those related to the other methods. They can reduce the path length by 4% (Part A), 9% (Part B) and 7% (Part C) compared with the corresponding parameters of the method in Ref. [12] (symbolled as SSV$_M$). It is pointed out that because the value of radial depth of cut in the comparison experiment is close to the optimal optimization result, the improvement is not very obvious, compared with the results corresponding to the existing selection method involving SSV. As for constant spindle speed (symbolled as CSS), whose parameters are selected by stability analyses for different radial and axial depths of cut, the optimization of proposed method can respectively guarantee 30%, 38% and 29% reductions of path length for each part.

Fig. 8 shows the actual scheduled results of single layer trajectory for Part B based on the final optimized parameters from the proposed method. Compared with the scheduled results using the constant feedrate method, the machining time is obviously reduced (from 30.46 s to 26.53 s) by 13%. Fig. 9 shows the feed per tooth based on the scheduled feedrate. It is found that the variable feedrate scheduling method can eliminate the influence of variable spindle speed on feed per tooth and achieve the constant maximum feed per tooth. Therefore, the influence of variable amplitude RVA on feed per tooth, which is not considered in the existing optimization method, can be eliminated through

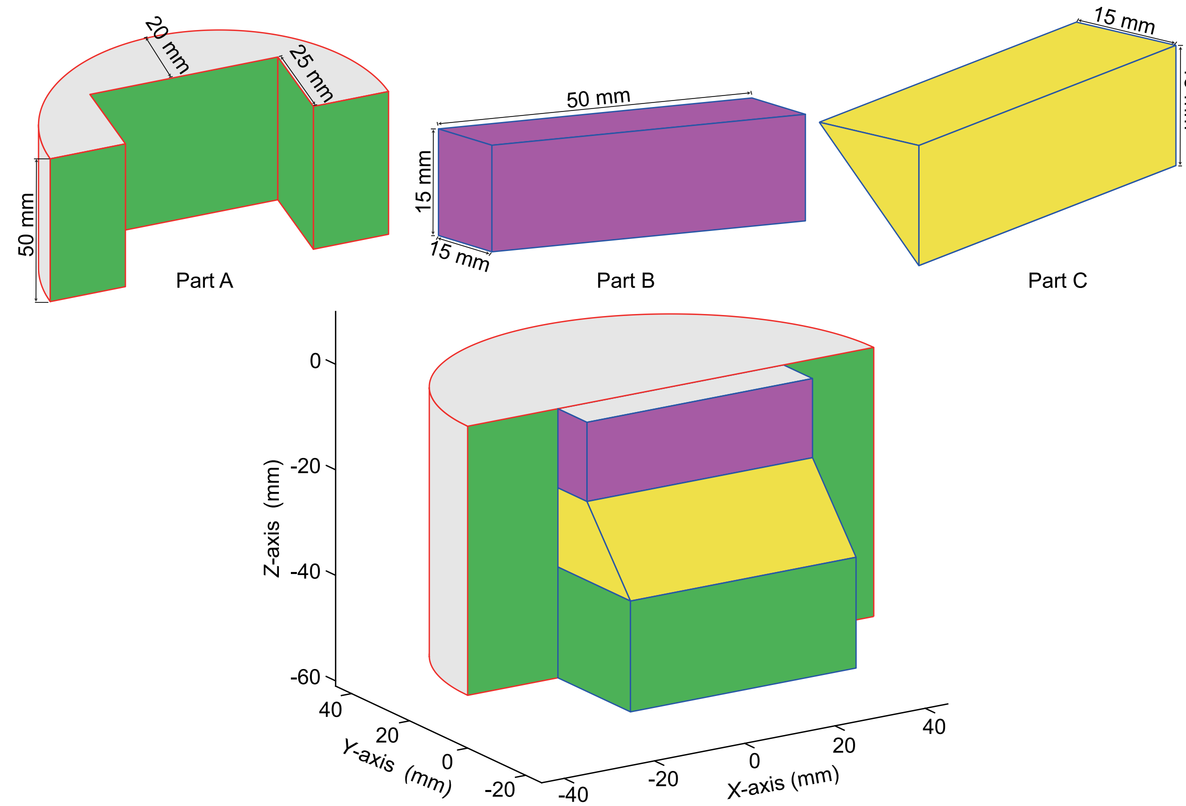

Fig. 7. The required inclined table workpiece with three cutting areas: Part A, Part B and Part C.

Table 2
Optimized parameters in relation to the inclined table workpiece with the proposed method.

Area	a_e (mm)	a_p (mm)	RVF	RVA	m	Path length (m)
Part A	1.539	1.515	0.0150	0.1201	33	51.28
	2	1.220	0.0130	0.1332	41	49.27
	2.5	1	0.0145	0.1285	50	47.76
	3.333	0.781	0.0145	0.1285	63	47.49
	4	0.658	0.0130	0.1300	76	48.26
	5	0.532	0.0145	0.1285	94	46.47
	6.67	0.394	0.0145	0.1285	127	49.22
Part B	1.5	1.5	0.0150	0.1201	10	5.8
	1.67	1.364	0.0150	0.1201	11	5.74
	2.143	1.154	0.0145	0.1285	13	5.28
	2.5	1	0.0145	0.1285	15	5.22
	3.75	0.682	0.0120	0.1340	22	5.1
	5	0.536	0.0145	0.1285	28	4.87
	7.5	0.334	0.0145	0.1285	45	5.22
Part C	1.414	1.515	0.0150	0.1201	7	3.65
	1.768	1.326	0.0145	0.1285	8	3.25
	3.033	0.816	0.0120	0.1340	13	3.25
	4.243	0.624	0.0130	0.1300	17	3.07
	5.303	0.505	0.0145	0.1285	21	3.07
	7.071	0.366	0.0145	0.1285	29	3.42

the variable feedrate scheduling method to simplify the optimization procedure.

For the first set of experiments, the chatter suppression of SSV is verified to guarantee stable milling. Fig. 10 is the result of stability analyses including constant spindle speed and the parameter optimization results of SSV for the three parts, respectively. It can be found that all stable machining parameters obtained by SSV parameters optimization method (squares) generate larger axial depth of cut than that of constant spindle speed (circles). It expresses the effectiveness of SSV on chatter suppression. More experimental results for chatter suppression based on SSV can be found in Appendix A.

The experiments of actually machining workpiece are carried out after the stability verification. The machining parameters obtained from different methods are shown in Table 2. Fig. 11 shows the machined

Table 3
Optimized parameters in relation to the inclined table workpiece with different methods.

Method	Area	a_e (mm)	a_p (mm)	RVF	RVA	Path length (m)	Improvement rate
	Part A	5	0.532	0.0145	0.1285	46.47	–
SSV_O	Part B	5	0.536	0.0145	0.1285	4.87	–
	Part C	4.243	0.624	0.0145	0.1285	3.07	–
	Part A					48.26	4%
SSV_M	Part B	4	0.66	0.0130	0.1300	5.34	9%
	Part C					3.31	7%
	Part A					66.06	30%
CSS	Part B	4	0.45	–	–	7.89	38%
	Part C					4.64	29%

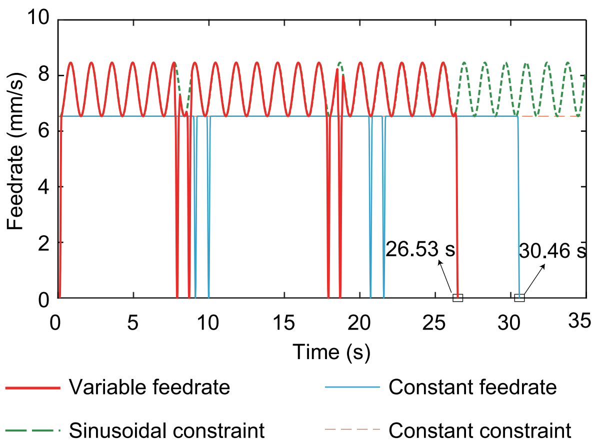

Fig. 8. The sinusoidal feedrate scheduling results with the variable feedrate (heavy solid line) and the constant feedrate (fine solid line) for a single layer trajectory of Part B. The actual constraint is expressed by heavy dashed line and the fine dashed line is the constraint of constant feedrate.

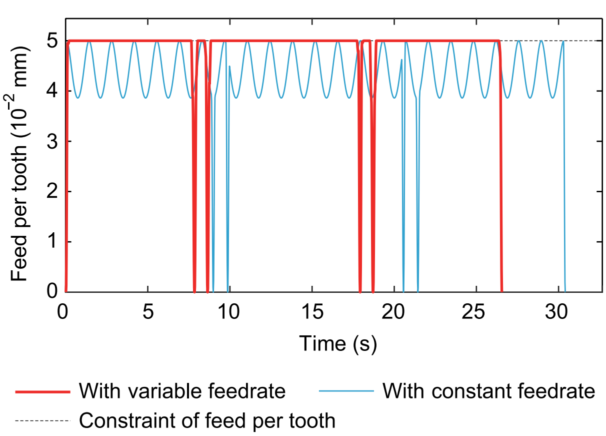

Fig. 9. The comparison of two sets of feeds per tooth for the machining processes with variable feedrate (heavy solid line) or the constant feedrate (fine solid line). The constraint of feed per tooth is expressed by dashed line.

workpieces and their surfaces based on different parameters obtained from different methods (SSV_O, SSV_M and CSS). It can be found that the surface quality of three machined parts is at the same level. Especially, the most surfaces corresponding to the proposed method (SSV_O) even produce the smallest roughness. It can be clearly seen that the surface quality of the three cuts are at the same level. Above results verify that the proposed optimization algorithm can decrease the length of tool path to improve machining productivity without decreasing the machining precision. Besides surface, the results of tracking errors of the X-axis, which are collected by the real-time control board, are shown in Appendix A.

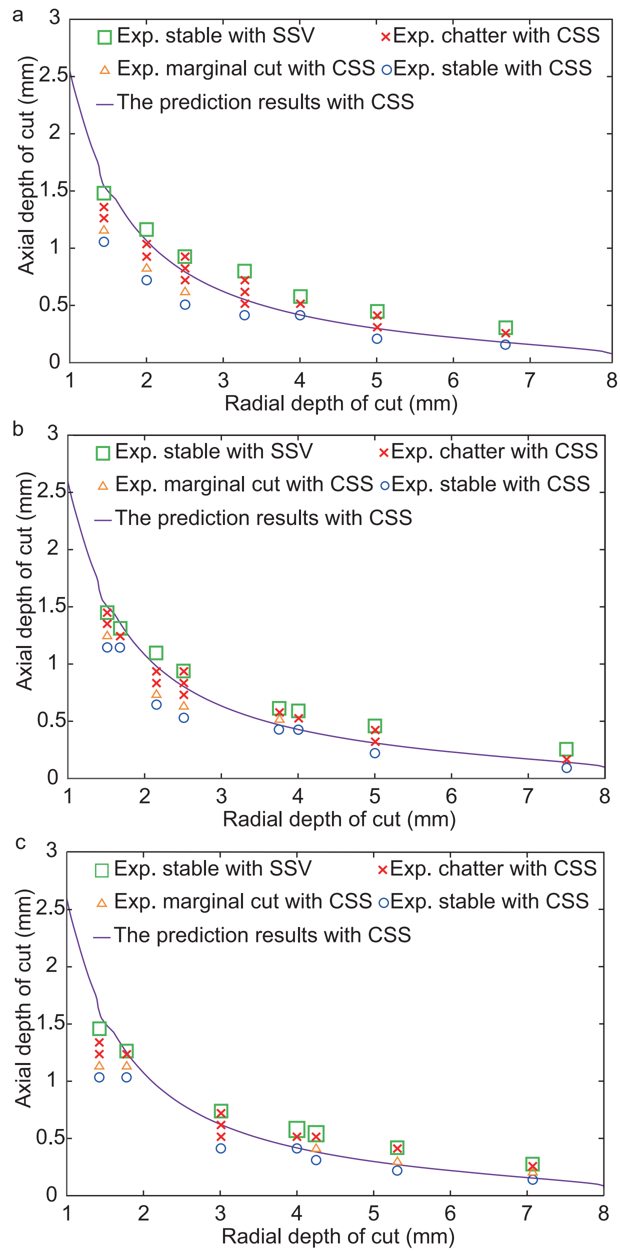

Fig. 10. The optimized results and milling stability experimental results for (a) Part A, (b) Part B and (c) Part C. The squares and circles are the stable milling processes with SSV and CSS, respectively. The results of unstable and the marginal depth with CSS are marked with crosses and asterisks, respectively.

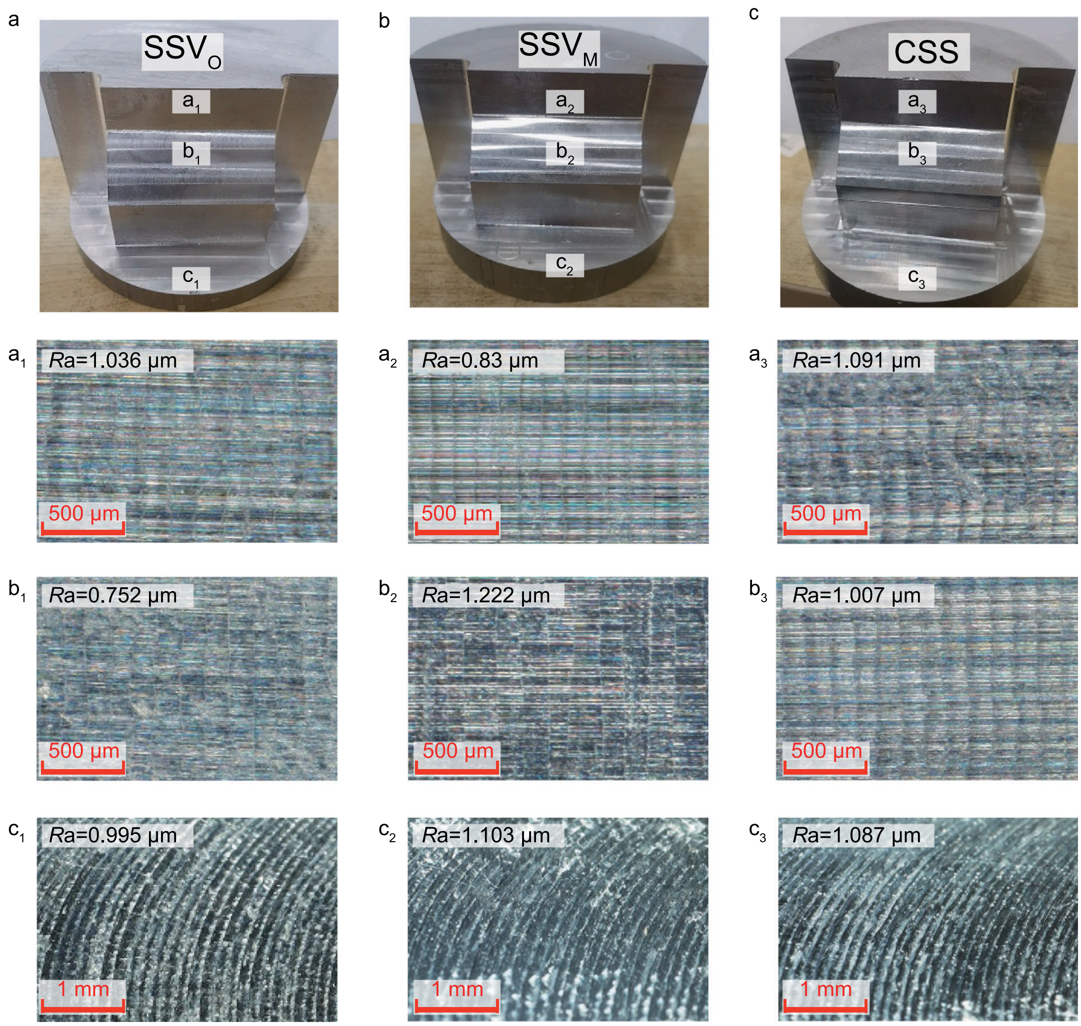

Fig. 11. The machined workpiece with different parameters by using (a) the proposed method (SSV_O), (b) the existing method (SSV_M) and (c) CSS and their surfaces.

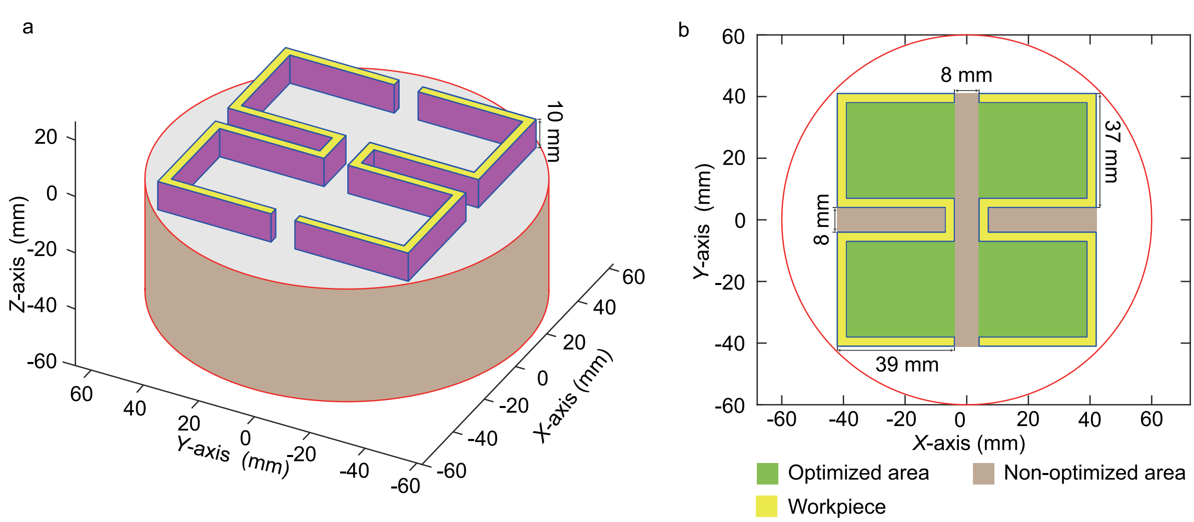

Fig. 12. The pocket workpiece together with the cutting area.

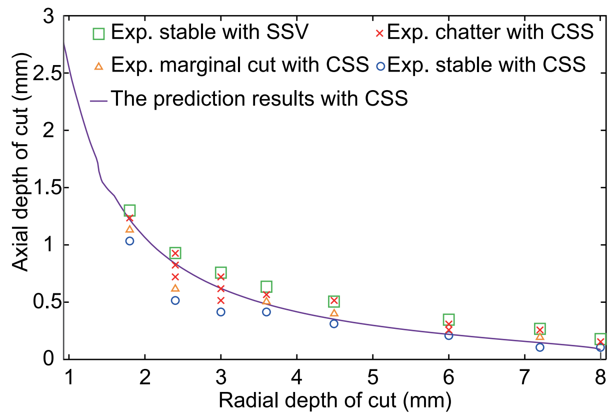

Fig. 13. The optimized results and stability experimental results for different milling parameters of pocket workpiece. The squares and circles are the stable millings with SSV and CSS, respectively. The results of unstable and marginal depth with CSS are marked with crosses and asterisks, respectively.

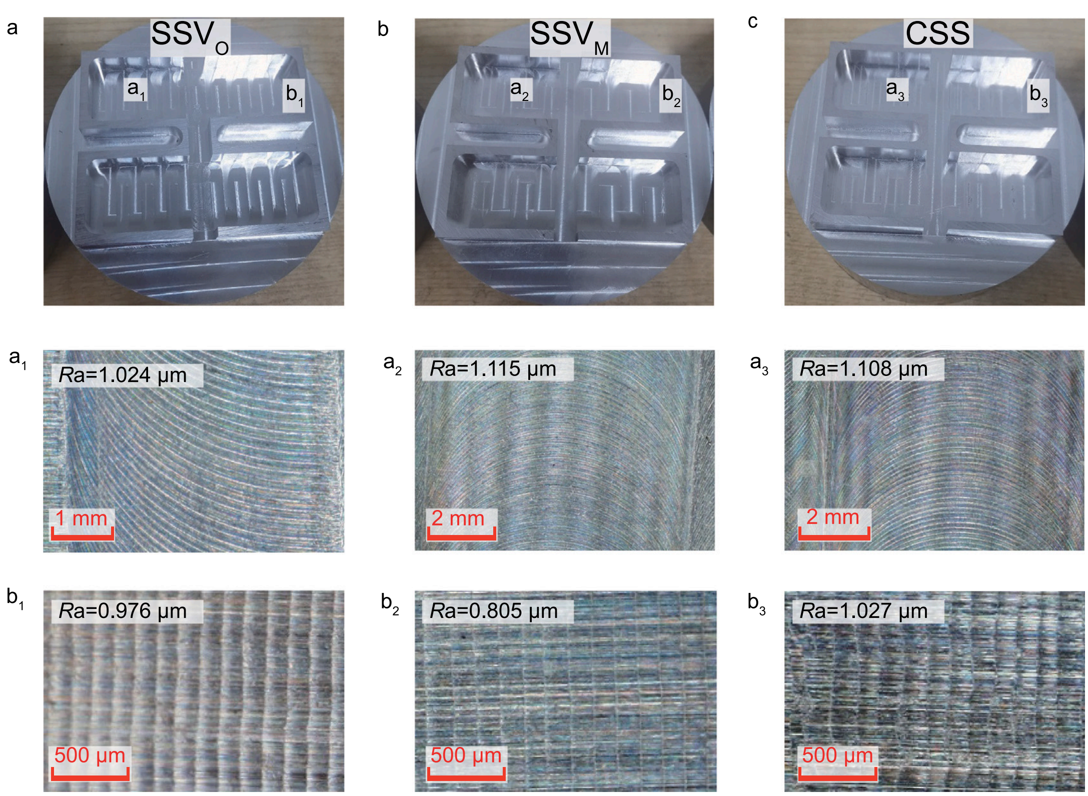

Fig. 14. The machined pocket workpieces with different parameters by using (a) the proposed method (SSV_O), (b) the existing method (SSV_M) and (c) CSS and their surface results.

3.2. Experimental verification for pocket workpieces

In this section, another type of workpiece, i.e. the part with pockets, which is shown in Fig. 12, is used to verify the improvement of proposed optimization method. The radial depth of cut in the non-optimized area is chosen as 8 mm. The initial radial depth of cut in the area to be optimized is also chosen as 8 mm. The optimized results of the parameter combination are listed in Table 4, in which the set of parameters marked with yellow squares is the final optimization result. As for comparison, the existing method, which can only optimize the SSV parameters for the maximum axial depth of cut, is also used with the radial depth of cut a_e = 8 mm. Comparison of the optimization results from different methods is listed in Table 5. It can be found that the path length corresponding to the proposed method (SSV_O) is obviously shorter than the length based on the parameters associated with the existing method (SSV_M). The proposed method, which considers the influence of radial depth of cut, can achieve the reduction of path length by 20%. Combined with the parameters from stability analyses of constant spindle speed (CSS), the optimal parameters for SSV can achieve the improvement by up to 37%.

Fig. 13 is the results of stability verification experiments for different processes with SSV and constant spindle speed. All parameter results for every radial depth of cut, which are based on SSV, can achieve stable milling, and then improve the axial depth of cut. Besides,

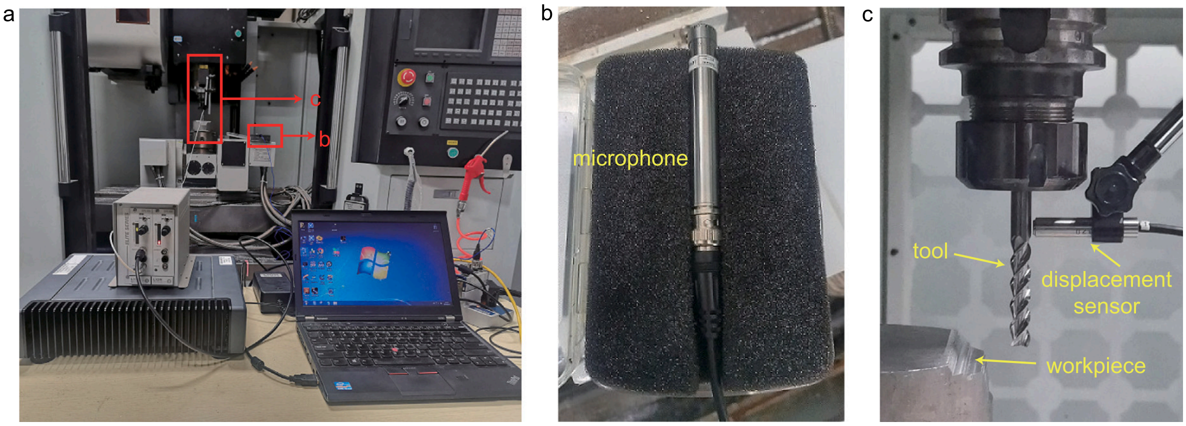

Fig. 15. The experimental setup to measure sound signals and displacement signals. The sound signals and the displacement signals are measured by (b) microphone and (c) capacitance displacement sensor, respectively.

Table 4
Optimized parameters for the pocket workpiece with the proposed method.

a_e (mm)	a_p (mm)	RVF	RVA	m	Path length (m)
1.8	1.25	0.0150	0.1201	8	20.42
2.4	1	0.0145	0.1285	10	19.5
3	0.833	0.0100	0.1351	12	18.95
3.6	0.714	0.0145	0.1285	14	18.58
4.5	0.588	0.0130	0.1332	17	18.21
6	0.435	0.0120	0.1340	23	18.39
7.2	0.357	0.0145	0.1285	28	18.58
8	0.27	0.0130	0.1332	37	22.57

Table 5
Optimal parameters for pocket workpiece from different methods.

Method	a_e (mm)	a_p (mm)	RVF	RVA	Path length (m)	Improvement rate
SSV_O	4.5	0.588	0.0130	0.1332	18.21	–
SSV_M	8	0.27	0.0130	0.1332	22.72	20%
CSS	8	0.2	–	–	28.7	37%

both Figs. 10 and 13 show that as RDC increases, the difference between SSV and CSS reduces. The reason is as follows. The critical stable ADC gradually reduces with RDC in both cases of SSV and CSS. As a result, the absolute difference between SSV and CSS is correspondingly reduced. However, although the absolute difference is reduced, the improvement percentage of SSV relative to CSS does not allow the decreasing tendency. With respect to an extreme case of slot milling, the improvement percentage of ADC is up to 35% (from 2 mm to 2.7 mm), as shown in Table 5. From Table 5 it can be seen that the machining trajectory, which is obtained for slot milling by the proposed method, is shortened from 28.7 m to 22.72 m.

Finally, three sets of optimized parameters shown in Table 5 are used to machine the pocket workpiece. Fig. 14 shows the machined workpieces corresponding to different methods. The roughnesses of all the machined surfaces are very similar and they are nearly 1 μm. Both the small roughnesses and glaze surfaces verify the stable machining of the three sets of parameters. Other experiment results, including scheduled feedrate results, feed per tooth and tracking errors, can be founded in Appendix B. All experiment results indicate that the proposed parameters optimization method can achieve shorter path length and higher machining efficiency, and simultaneously guarantee the machining quality.

4. Conclusions

This work optimized both the machining parameters (RDC and ADC) and SSV parameters (RVF and RVA) in milling process. The length of path, other than the axial depth of cut, is set as the optimization objective. The influence of spindle speed variation on the feed per tooth is also considered, and it is eliminated by a C^3 continuous variable feedrate scheduling method. An open-architecture CNC machine tool with self-designed controllers is developed to carry out a series of milling experiments for the verification of the proposed method. The main conclusions are obtained as follows.

(1) The combined optimization of ADC and RDC achieves an obvious reduction of tool path than the existing SSV optimization method, which only optimized ADC. The optimized parameters for every step are chosen as the fewer axial or radial cutting layers, and this significantly reduces the optimization loads for SSV. Experimental results verify that the actual lengths of different tool paths produced by the proposed method is decreased by 4%, 9%, 7% and 20%, respectively, compared with existing SSV optimization method.
(2) The stability for every set of parameters obtained by the proposed method is verified by milling experiments. It thus reveals the effectiveness of the SSV methods on chatter suppression. Compared with the machining processes with constant spindle speed, the proposed SSV optimization method achieves the reduction of tool path lengths by 30%, 38%, 29% and 37% for the different machining trajectories.
(3) The optimization of feed per tooth influenced by RVA is successfully eliminated by a C^3 continuous variable feedrate scheduling

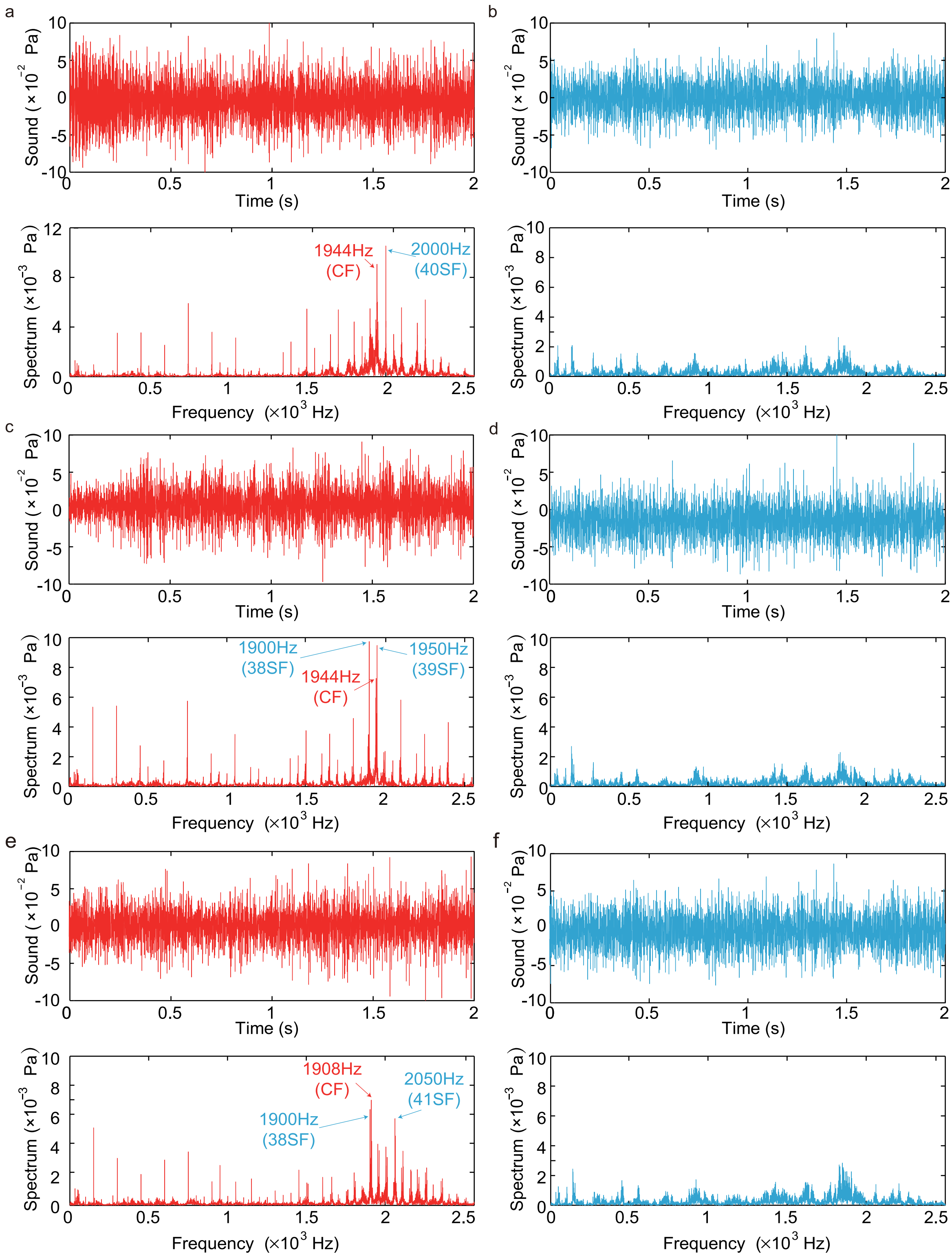

Fig. 16. Sound signals together with their spectra for the cuts during different cases. The results for CSS with (a) a_e=4 mm, a_p=0.6 mm; (c) a_e=5 mm, a_p=0.5 mm; (e) a_e=4.243 mm, a_p=0.6 mm. The results for SSV with (b) a_e=4 mm, a_p=0.66 mm, RVA=0.13,RVF=0.013; (d) a_e=5 mm, a_p=0.536 mm, RVA=0.145,RVF=0.01285; (f) a_e=4.243 mm, a_p=0.624 mm, RVA=0.145, RVF=0.01285. Here, symbol 'CF' is the chatter frequency and symbol 'SF' means the frequency of spindle.

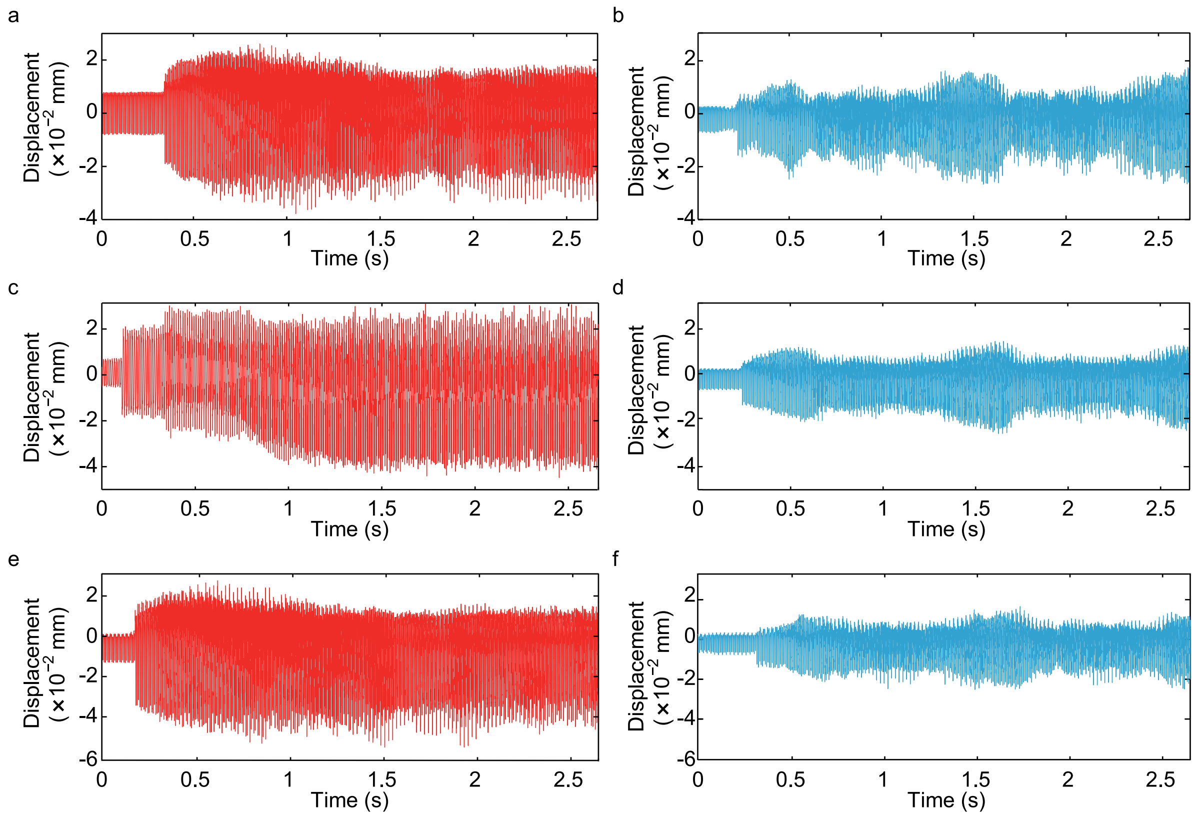

Fig. 17. The measured results of displacement signals for the milling experiments. The unstable milling results for CSS with (a) a_e=4 mm, a_p=0.6 mm; (c) a_e=5 mm, a_p=0.5 mm; (e) a_e=4.243 mm, a_p=0.6 mm. The stable experiment results for SSV with (b) a_e=4 mm, a_p=0.66 mm, RVA=0.13,RVF=0.013; (d) a_e=5 mm, a_p=0.536 mm, RVA=0.145,RVF=0.01285; (f) a_e=4.243 mm, a_p=0.624 mm, RVA=0.145, RVF=0.01285.

method. Experiments reveal that for the used two types of workpieces, the scheduled variable feedrate can achieve the constant feed per tooth with SSV, and thus, it realizes reducing the actual machining time by 13% than the SSV process with a constant feedrate.

CRediT authorship contribution statement

Min Wan: Conceptualization, Idea proposal, Investigation, Methodology, Resources, Supervision, Data curation, Writing – review & editing, Funding acquisition. **Xue-Bin Qin:** Conceptualization, Idea execution, Investigation, Methodology, Validation, Data curation, Coding, Experimental verification, Writing – original draft. **Jia Dai:** Methodology, Code checking, Visualization, Experimental verification. **Wei-Hong Zhang:** Conceptualization, Validation, Resources, Experimental proposal, Supervision. **Xiao-Ling Sun:** Experimental proposal checking, Experimental validation, Data curation.

Declaration of competing interest

The authors declare that they have no known competing financial interests or personal relationships that could have appeared to influence the work reported in this paper.

Acknowledgements

This research has been supported by the National Natural Science Foundation of China under Grant no. 51975481.

Appendix A. More experimental results in relation to Section 3.1

The results of sound signals and displacement signals for CSS and SSV, and the tracking errors which were acquired during machining the inclined table workpieces of Section 3.1 are displayed here as supplementary contents.

Sound signals measured through a microphone and a software CUTPRO^{TM} (see Fig. 15a,b) is a means to determine whether chatter occurs or not. Based on the spectra obtained from Fourier transformation, the milling process can be judged as the cut with chatter if the spectra have peaks around the natural frequencies of cutting system, but do not overlap with the harmonics of spindle passing frequencies (SPF). However, stable cuts can be determined if strongly excited spectra are distributed in the multiples of SPF. Fig. 16 shows the sound signals and their spectra for different machining parameters whether with SSV or not. The machining parameters of SSV are set as the same as the parameters optimized by the proposed method and the existing method, respectively. Among them, Fig. 16a,c,e are the milling results of CSS, while Fig. 16b,d,f are the experiment results of SSV. Every set of them has the same radial depth of cut but the axial depth of cut with SSV is larger than that with CSS. For the results of Fig. 16a,c,e, which corresponds to CSS, it can be found that chatter occurs because of the obvious chatter frequency. However, the results corresponding to SSV with the larger axial depth of cut and same radial depth of cut, including Fig. 16b,d,f, show much lower spectra than those of CSS. It means that SSV shows an effective chatter suppression. Furthermore, Fig. 17 shows the displacement signals, which are obtained by a capacitance displacement sensor, as shown in Fig. 15c. It can be found that the displacement of SSV is obviously smaller than the displacement of CSS. At last, the machining surfaces are displayed in Fig. 18. Compared with

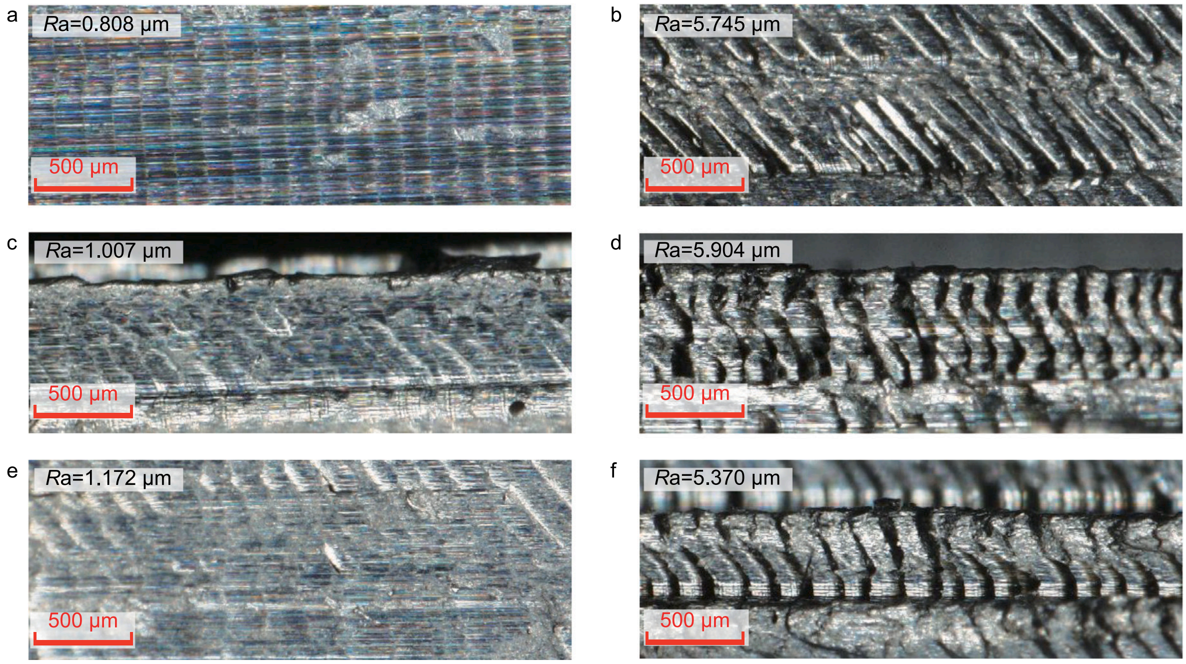

Fig. 18. The milling surfaces of the stability verification experiments. The milling surfaces for SSV with (a) a_e=4 mm, a_p=0.66 mm, RVA=0.13,RVF=0.013; (c) a_e=5 mm, a_p=0.536 mm, RVA=0.145,RVF=0.01285; (e) a_e=4.243 mm, a_p=0.624 mm, RVA=0.145, RVF=0.01285. The milling surfaces for CSS with (b) a_e=4 mm, a_p=0.6 mm; (d) a_e=5 mm, a_p=0.5 mm; (f)a_e=4.243 mm, a_p=0.6 mm.

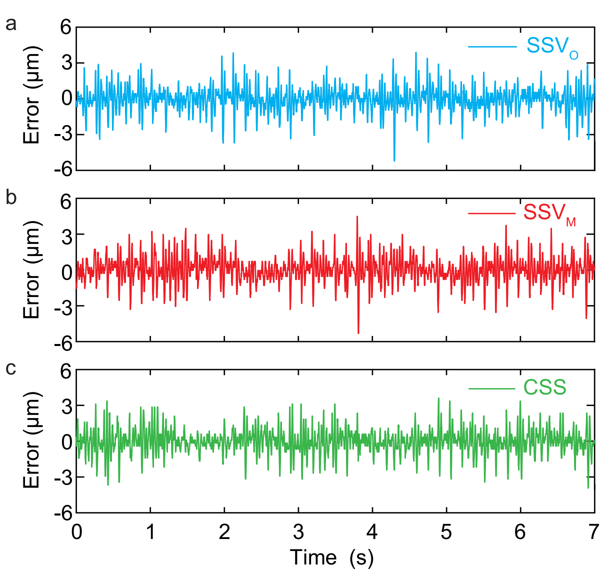

Fig. 19. The tracking error of X-axis for the experiments with (a) the proposed method (SSV$_O$), (b) the existing method (SSV$_M$) and (c) constant spindle speed (CSS).

the surfaces from CSS, the surfaces of SSV are smoother and their values of roughness are obviously smaller than those of CSS. On balance, all results about signals and surfaces can reveal that SSV can suppress chatter effectively and the machining parameters from the proposed optimization method can achieve stable milling.

The tracking errors of X-axis, which are collected by the real-time control board, are shown in Fig. 19. It can be clearly seen that the tracking errors of the three cuts are at the same level.

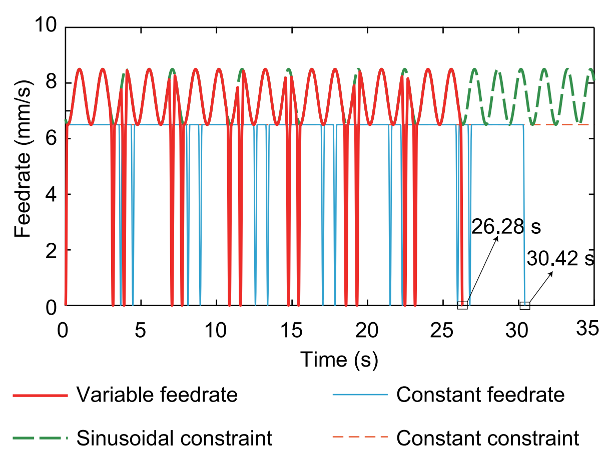

Fig. 20. The feedrate scheduling results based on the variable feedrate scheduling method (heavy solid line) and constant feedrate scheduling method (fine solid line) for part trajectory of optimized area. The constraints of two sets of results are expressed by heavy dashed line (variable feedrate) and fine dashed line (constant feedrate), respectively.

Appendix B. More experimental results in relation to Section 3.2

The scheduled feedrate and acquired tracking errors for pocketing workpiece in Section 3.2 are displayed in this appendix as supplementary.

Fig. 20 shows the feedrate scheduling results for the part trajectory of the optimized area. It can be found that the machining process with variable feedrate only needs 26.28 s, while the process with constant feedrate needs 30.42 s for the same trajectory, and the reduction of machining time is also higher than 13%. Fig. 21 displays the feed per tooth for the two sets of machining with variable feedrate and constant feedrate, respectively. The constant maximum feed per tooth verifies

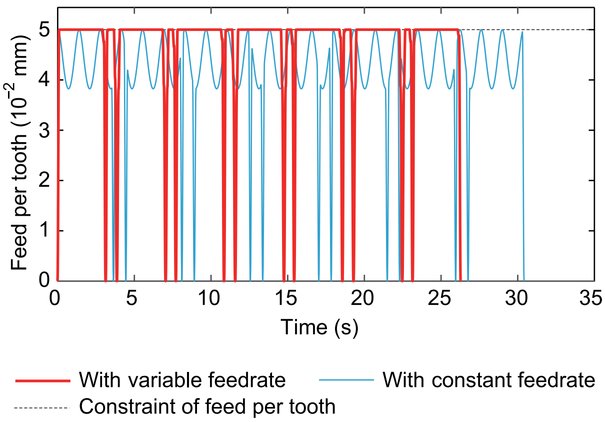

Fig. 21. The comparison of two sets of feeds per tooth for the machining processes with variable feedrate (heavy solid line) or the constant feedrate (fine solid line), respectively. The dashed line expresses the constraint of feed per tooth.

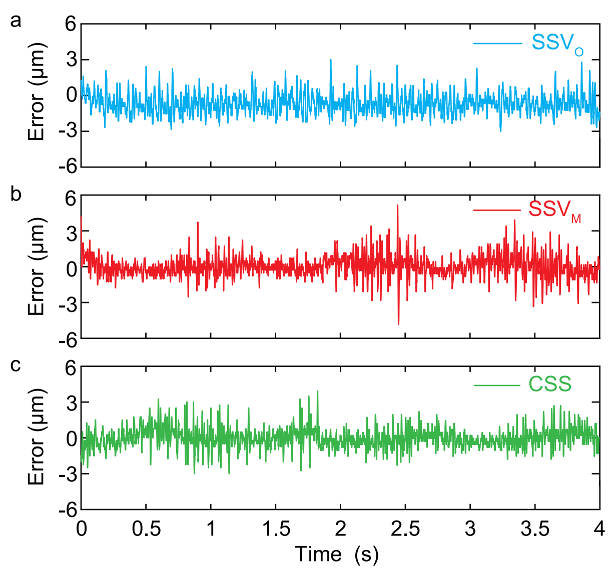

Fig. 22. The tracking error of Y-axis for the experiments by using (a) the proposed method (SSV$_O$), (b) the existing method (SSV$_M$) and (c) constant spindle speed (CSS).

the scheduled variable feedrate can eliminate the influence of variation frequency for spindle speed on the actual feed per tooth, and thus achieve high machining efficiency.

Fig. 22 shows the tracking errors of Y-axis, which are measured during different machining processes. They also reveal that the machining qualities of different workpieces machined with different parameters are indistinguishable.

References

[1] Y. Altintas, E. Budak, Analytical prediction of stability lobes in milling, CIRP Ann 44 (1995) 357–362.

[2] T. Insperger, G. Stepan, Updated semi-discretization method for periodic delay-differential equations with discrete delay, Internat J Numer Methods Engrg 61 (2004) 117–141.

[3] M. Wan, Y. Li, D.-Y. Wen, W.-H. Zhang, Y. Yang, On cutting process damping for small cutters by including the influences of the dead metal zone and elastic recovery, J Mater Process Technol 306 (2022) 117608.

[4] N. Sims, B. Mann, S. Huyanan, Analytical prediction of chatter stability for virable pitch and variable helix milling tools, J Sound Vib 317 (2008) 664–686.

[5] T. Takemura, T. Kitamura, T. Hoshi, Active suppression of chatter by programmed variation of spindle speed, J Japan Soc Precis Eng 41 (1975) 489–494.

[6] Y. Altintas, P.K. Chan, In-process detection and suppression of chatter in milling, Int J Mach Tools Manuf 32 (1992) 329–347.

[7] S. Seguy, G. Dessein, L. Arnaud, T. Insperger, Control of chatter by spindle speed variation in high speed milling, Adv Mater Res 112 (2010) 179–186.

[8] K.H. Hajikolaei, H. Moradi, G. Vossoughi, M.R. Movahhedy, Spindle speed variation and adaptive force regulation to suppress regenerative chatter in the turning process, J Manuf Process 12 (2010) 106–115.

[9] F. Kong, P. Liu, X. Zhao, Simulation and experimental research on chatter suppression using chaotic spindle speed variation, Trans ASME - J Manuf Sci Eng 133 (2011) 014502.

[10] G. Jin, H. Qi, Z. Li, J. Han, Dynamic modeling and stability analysis for the combined milling system with variable pitch cutter and spindle speed variation, Commun Nonlinear Sci Numer Simul 63 (2018) 38–56.

[11] L. Ding, Y. Sun, Z. Xiong, Active chatter suppression in turning by simultaneous adjustment of amplitude and frequency of spindle speed variation, Trans ASME - J Manuf Sci Eng 142 (2020) 021004.

[12] J. Niu, Y. Ding, L. Zhu, H. Ding, Stability analysis of milling processes with periodic spindle speed variation via the variable-step numerical integration method, Trans ASME - J Manuf Sci Eng 138 (2016) 114501.

[13] X. Dong, X. Shen, Z. Fu, Stability analysis in turning with variable spindle speed based on the resconstructed semi-discretization method, Int J Adv Manuf Technol 117 (2021) 3393–3403.

[14] Z. Wang, M. Rahman, Y. Wong, J. Sun, Optimization of multi-pass milling using parallel genetic algorithm and parallel genetic simulated annealing, Int J Mach Tools Manuf 45 (2005) 1726–1734.

[15] R.K. Agrawal, D. Pratihar, A. Roy Choudhury, Optimization of CNC isoscallop free form surface machining using a genetic algorithm, Int J Mach Tools Manuf 46 (2006) 811–819.

[16] A. Tang, Z. Liu, Three-dimensional stability lobe and maximum material removal rate in end milling of thin-walled plate, Int J Adv Manuf Technol 43 (2009) 33–39.

[17] C. Ozoegwu, S. Ofochebe, C. Ezugwu, Time minimization of pocketing by zigzag passes along stability limit, Int J Adv Manuf Technol 86 (2016) 581–601.

[18] S. Kumar, B. Singh, Stable cutting zone with improved metal removal rate in turning process, Int J Adv Manuf Technol 44 (2020) 129–147.

[19] B. Bergmann, S. Reimer, Online adaption of milling parameters for a stable and productive process, CIRP Ann 70 (2021) 341–344.

[20] K. Ringgaard, Y. Mohammadi, C. Merrild, O. Balling, K. Ahmadi, Optimization of material removal rate in milling of thin-walled structures using penalty cost function, Int J Mach Tools Manuf 145 (2019) 103430.

[21] C. Deng, J. Shu, Y. Ma, S. Lu, Y. Zhao, J. Miao, Multi-objective modelling and optimal parameter selection of a multi-pass milling process considering uncertain milling stability constraint, Int J Adv Manuf Technol 120 (2022) 6225–6240.

[22] A. Harun, Multiple optimization analysis of MRR, surface roughness, sound intensity, energy consumption, and vibration values in machinability of TC4 titanium alloy, Surf Rev Lett 28 (2021) 2150072.

[23] X. Zhang, T. Pan, A. Ma, W. Zhao, High efficiency orientated milling parameter optimization with tool wear monitoring in roughing operation, Mech Syst Signal Process 165 (2022) 108394.

[24] S. Seguy, T. Insperger, L. Arnaud, G. Dessein, G. Peigne, On the stability of high-speed milling with spindle speed variation, Int J Adv Manuf Technol 48 (2010) 883–895.

[25] C. Wang, X. Zhang, R. Yan, X. Chen, H. Gao, Multi harmonic spindle speed variation for milling chatter suppression and parameters optimization, Precis Eng 55 (2019) 268–274.

[26] X. Qin, M. Wan, W. Zhang, Y. Yang, Chatter suppression with productivity improvement by scheduling a C^3 continuous feedrate to match spindle speed variation, Mech Syst Signal Process 188 (2023) 110021.

[27] Y. Ding, J. Niu, L. Zhu, H. Ding, Numerical integration method for stability analysis of milling with variable spindle speeds, Trans ASME - J Vibr Acoust 138 (2016) 011010.